MPA 1286
May 2000

Spherically symmetric simulation with Boltzmann neutrino transport of core collapse and post-bounce evolution of a 15 $M_\odot$ star

Markus Rampp and Hans-Thomas Janka

Max-Planck-Institut für Astrophysik, Karl-Schwarzschild-Str. 1, 85741 Garching, Germany

Submitted to: *Astrophysical Journal, Letters*

DRAFT VERSION MAY 22, 2000
Preprint typeset using LaTeX style emulateapj

SPHERICALLY SYMMETRIC SIMULATION WITH BOLTZMANN NEUTRINO TRANSPORT OF CORE COLLAPSE AND POST-BOUNCE EVOLUTION OF A 15 $M_\odot$ STAR

MARKUS RAMPP[1] AND H.-THOMAS JANKA[1]

Draft version May 22, 2000

ABSTRACT

We present results of a spherically symmetric, Newtonian simulation of the core-collapse and post-bounce evolution of a 15 $M_\odot$ star with a 1.28 $M_\odot$ iron core. The time-, energy-, and angle-dependent transport of electron neutrinos (ν_e) and antineutrinos ($\bar{\nu}_e$) was treated with a new code which iteratively solves the Boltzmann equation and the equations for neutrino number, energy and momentum, including the effects of the motion of the stellar medium to order $O(v/c)$ in the fluid velocity v. The supernova shock expands to a maximum radius of 350 km instead of only ~ 240 km as in a comparable calculation with multi-group flux-limited diffusion (MGFLD) by Bruenn, Mezzacappa, & Dineva (1995). We explain this by stronger neutrino heating due to the more accurate treatment of the transport in our model. Nevertheless, shock expansion breaks down at 180 ms after bounce, and the shock finally recedes to a radius around 250 km (compared to ~ 170 km in the MGFLD run). The effect of an accurate neutrino transport is helpful, as expected, but not large enough to cause an explosion of the considered 15 $M_\odot$ star in spherical symmetry. Therefore postshock convection and/or an enhancement of the core neutrino luminosity by convection or reduced neutrino opacities in the neutron star seem necessary for neutrino-driven delayed explosions of such stars. We find that the electron fraction Y_e in the neutrino-heating region is larger than 0.5, which suggests that the overproduction problem of neutron-rich nuclei with mass numbers around $A \approx 90$ in the neutrino-heated ejecta is absent when ν_e and $\bar{\nu}_e$ spectra and luminosities are calculated with a Boltzmann solver.

Subject headings: supernovae: general — hydrodynamics — elementary particles: neutrinos

1. INTRODUCTION

The mechanism of supernova explosions of massive stars is still not satisfactorily understood. Detailed numerical models showed that the hydrodynamic shock front, which is launched when the collapsing stellar core bounces abruptly by the stiffening of the equation of state (EoS) at nuclear matter densities, cannot propagate out promptly but stalls because of severe energy losses due to photodisintegration of iron-group nuclei and neutrino emission from the shock-heated matter (Bowers & Wilson 1980; Bruenn 1985, 1989a,b; Myra et al. 1987). Early suggestions that energy deposition by neutrinos, which carry off 99% of the energy released during stellar core collapse and neutron star formation, might play a crucial role for the explosion reach back to Colgate & White (1966). The modern version of the neutrino-driven "delayed" explosion mechanism is due to Wilson (1985), who found that neutrino energy deposition can revive the stalled shock on a time scale of several hundred milliseconds after core bounce (Bethe & Wilson 1985). Because of the complexity of the involved physics and the low efficiency of the neutrino energy transfer it remained unclear for many years whether the explosions are sufficiently energetic and whether the delayed mechanism works for a larger range of stellar masses (Wilson et al. 1986; Bruenn 1993). Recognizing that neutron-finger convection in the newly formed neutron star could increase the neutrino luminosities, Wilson & Mayle (1988, 1993) managed to obtain healthy explosions. However, the question of neutron star convection is still not finally settled and currently it is not clear whether neutron-finger instabilities or Ledoux convection (Burrows 1987, Pons et al. 1999) or quasi-Ledoux convection (Keil, Janka, & Müller 1996; Janka & Keil 1998) or none (Bruenn et al. 1995; Bruenn & Dineva 1996; Mezzacappa et al. 1998a) occur and how they affect the explosion mechanism.

Multi-dimensional hydrodynamic models (Herant, Benz, & Colgate 1992; Herant et al. 1994; Miller, Wilson, & Mayle 1993; Burrows, Hayes, & Fryxell 1995; Janka & Müller 1995, 1996; Mezzacappa et al. 1998b), however, have convincingly demonstrated the existence and the importance of convective overturn in the neutrino-heating region below the supernova shock. Driven by a negative entropy gradient which emerges behind the weakening prompt shock and is enhanced by the neutrino energy deposition, the convective motions transport energy from around the gain radius, where neutrino heating is strongest, to the shock, thus raising the postshock pressure and pushing the shock farther out. At the same time, cold, low-entropy matter is advected downward where it can readily absorb energy from the upstreaming neutrinos. These hydrodynamic instabilities have a bearing on the measured kick velocities of pulsars and the anisotropies observed in many supernovae. They are essential to understand the production of radioactive elements in the vicinity of the nascent neutron star and their large-scale mixing into the hydrogen and helium layers of the exploding star (Kifonidis et al. 2000).

All multi-dimensional simulations have so far been carried out with serious simplifications to the treatment of the neutrino transport. Even the most advanced spherically symmetric post-bounce models have only employed MGFLD (Bruenn 1993, Bruenn et al. 1995) until recently. The significance of an accurate description of the neutrino luminosities, neutrino spectra and the angular distribution of the neutrinos in the context of the delayed explosion mechanism, however, has long been recognized (Janka 1991, Messer et al. 1998, Yamada, Janka, & Suzuki 1999, Burrows et al. 2000). It is therefore a natural step that a new generation of supernova models will employ schemes based on a solution of the Boltzmann equation for the neutrino transport. In fact, Mezzacappa et al. (2000) have published re-

[1]Max-Planck-Institut für Astrophysik, Karl-Schwarzschild-Str. 1, D-85741 Garching, Germany; mjr@mpa-garching.mpg.de; thj@mpa-garching.mpg.de

sults of a simulation for a 13 $M_\odot$ star which demonstrate that a more accurate handling of the transport can make a qualitative change to the outcome of the simulations. However, they considered a model with an exceptionally small iron core of only 1.17 $M_\odot$ (Nomoto & Hashimoto 1988) and the explosion energy was very low, only 0.41×10^{51} erg at the end of their simulation at a post-bounce time of about 0.6 s. The growth rate of this energy of 0.05×10^{51} erg per 100 ms cannot easily be extrapolated in time and will probably not increase the explosion energy significantly, because the density around the mass cut drops rapidly and the heating region is evacuated by the developing bifurcation between neutron star and ejecta. Moreover, a general relativistic treatment of hydrodynamics and neutrino transport is likely to reduce the explosion energy.

In this *Letter* we present results for a Newtonian simulation of a 15 $M_\odot$ star with a 1.28 $M_\odot$ iron core (Woosley & Weaver 1995) which show that an accurate neutrino transport does not produce an explosion for this star in spherical symmetry.

2. NUMERICAL METHODS

We have developed a new code which determines the neutrino phase-space distribution by iteratively solving the radiation moment equations for neutrino energy and momentum coupled to the Boltzmann transport equation. The transport takes into account effects due to the motion of the stellar medium to order $O(v/c)$ and determines the neutrino quantities in a comoving frame of reference (Rampp 2000; Rampp & Janka 2000, in preparation). The option is implemented to switch to a general relativistic treatment. The angle dependence of the distribution function is accounted for by the use of a grid of tangent rays which exploits spherical symmetry. Closure of the set of moment equations is achieved by a variable Eddington factor calculated from the solution of the Boltzmann equation, and the integro-differential character of the latter is tamed by making use of the integral moments of the neutrino distribution as obtained from the moment equations. The method is similar to the one described by Burrows et al. (2000). In order to fulfill lepton number conservation, we employ additional moment equations for neutrino number density and number flux. Severe time step restrictions are avoided and proper establishment of equilibrium is ensured by integrating the set of transport equations implicitly in time. The stiff character of the source terms for neutrino energy and lepton number requires a simultaneous implicit update of the temperature and electron fraction of the stellar medium.

The neutrino transport is coupled to the hydrodynamics code *Prometheus*, which integrates the continuity equations for mass, momentum, energy and particle species in a conservative way on a moving radial grid by explicit time stepping. The integration is accurate to second order in space and time. Shocks are particularly well treated by solving local Riemann problems at the zone interfaces (Fryxell, Müller & Arnett 1989). The source terms for energy and momentum due to gravity and neutrinos, and for lepton number due to neutrino emission/absorption are handled by an operator-splitting technique. The stellar background and the neutrino component are evolved on different radial grids and with different time steps, which are constrained by changes per transport time step (which is larger than the CFL-limited time step of the hydrodynamics) of at most 10% for the neutrino quantities and 5% for the fluid quantities. Interpolation between both grids is done in a conservative manner.

We used the EoS of Lattimer & Swesty (1991) (with nuclear incompressibility modulus of $K = 180$ MeV) which is extended to densities and temperatures below the regime of nuclear statistical equilibrium by an ideal gas equation of state, corrected for Coulomb-lattice effects, that includes arbitrarily relativistic and degenerate electrons and positrons, photons, and a mixture of predefined nuclear species. Nuclear burning was not taken into account in the present simulation.

The hydrodynamics was solved on a grid with 400 radial zones out to 20000 km, which were moved with the infalling matter during core collapse and kept fixed later. For the transport we used a Eulerian grid with 210 geometrically spaced radial zones, 230 tangent rays and 27 energy bins geometrically distributed between 0 and 380 MeV, the zone center of the first zone being at 1 MeV. The quality of the energy conservation limits the error in the net energy deposition by neutrinos to $< 5 \times 10^{49}$ erg, and lepton number is globally conserved to better than 0.1%.

The present simulation includes only ν_e and $\bar{\nu}_e$. The corresponding rates for charged-current reactions with nucleons and nuclei, neutral-current scattering off nucleons and nuclei, and neutrino-electron scattering were taken from Bruenn (1985), Mezzacappa & Bruenn (1993) and Bruenn & Mezzacappa (1997). We neglect production and annihilation of $\nu_e\bar{\nu}_e$ pairs, which are of minor importance compared to the charged-current reactions with nucleons. A detailed comparison of core-collapse results with published models of Bruenn & Mezzacappa (1997) showed excellent agreement. Disregarding muon and tau neutrinos and antineutrinos and $\nu_e\bar{\nu}_e$ pair processes has virtually no effect on the explosion mechanism (see Bruenn 1993) and we think (and will argue below) that adding muon and tau neutrinos and antineutrinos would most likely make an explosion harder as does the inclusion of general relativistic effects (see Fryer 1999).

3. RESULTS

Figure 1 shows the trajectories of selected mass shells as a function of time from the beginning of our simulation. The bounce shock forms 211.6 ms after the onset of the collapse at a radius of 12.5 km with an enclosed mass of ~ 0.62 $M_\odot$. The central density at this time is $\rho_c = 3.3 \times 10^{14}\,\mathrm{g\,cm^{-3}}$ (cf. Bruenn & Mezzacappa 1997). About 25 ms after bounce the shock crosses the infalling iron-silicon interface at a radius of 110 km. By the rapid accretion of mass with a rate $\dot{M}$ (see Fig. 2; note that $\dot{M}$ is measured at the shock radius R_s) the shock is pushed out to ~ 240 km within the next 100 ms. When the accretion rate drops significantly at ~ 120 ms after bounce, neutrino heating is able to support further shock expansion to a radius of 350 km. After some time, however, the shock starts to retreat again and finally turns into a standing accretion shock around 250 km, still within the collapsing silicon shell of the progenitor star. No indication for the possibility of an explosion was visible when the simulation was terminated at 350 ms after bounce. At this time the shock enclosed a mass of 1.5 $M_\odot$.

The overall evolution of the model in our simulation is very similar to that of model WPE15ls(180)Newt20 in Bruenn et al. (1995), who used a MGFLD treatment of the neutrino transport. The most obvious difference is a larger maximum radius of the shock, 350 km compared to only ~ 240 km in the calculation by Bruenn et al. (1995). Also, the shock is able to stay near its maximum radius for a longer time and afterwards does not recede as far as in model WPE15ls(180)Newt20. We explain this difference by a stronger heating due to ν_e and $\bar{\nu}_e$ absorption in the postshock medium in our simulation with the more accurate Boltzmann transport. The ν_e and $\bar{\nu}_e$ luminosities and rms ener-

gies, defined as the root of the mean squared energy, at 1000 km are shown as functions of time in Fig. 2. The prompt ν_e burst with a peak luminosity of $L_{\nu_e} = 3.36 \times 10^{53}\,\mathrm{erg\,s^{-1}}$ arrives at this radial position only ~ 6 ms after core bounce. About 50 ms after bounce the ν_e and $\bar{\nu}_e$ luminosities have become roughly equal with a fairly stable value of $(2.5\text{–}3) \times 10^{52}\,\mathrm{erg\,s^{-1}}$. By the end of our simulation they begin to decrease slowly, different from the mean energies, which show a gradual rise and reach 11.2 MeV for ν_e and 15.5 MeV for $\bar{\nu}_e$ when the simulation was stopped.

In Fig. 3 we present profiles of the net energy deposition rate by ν_e and $\bar{\nu}_e$ reactions, of the electron fraction Y_e and of the entropy per baryon as obtained in the simulation for times 330 ms, 380 ms and 561 ms. The gain radius, below which net neutrino cooling and above which net neutrino heating occurs, is at 120–140 km (see also Fig. 1). Maximum heating rates are reached somewhat outside the gain radius and are up to $\sim 120\,\mathrm{MeV\,s^{-1}}$ per baryon. The cooling rate below the gain radius is typically around $50\,\mathrm{MeV\,s^{-1}}$ per baryon, but can exceed $200\,\mathrm{MeV\,s^{-1}}$ per baryon at late times. Maximum entropies around 13 k_B per nucleon are reached at the end of the simulation, when the density behind the shock is lowest because of the decreasing mass accretion rate. The negative gradient of the entropy profile is growing with time and indicates the instability against convective overturn of the region between maximum heating and supernova shock. We point out that in this layer of net energy deposition by ν_e and $\bar{\nu}_e$, the electron fraction Y_e climbs to values *larger* than 0.5. Values $Y_e > 0.5$ are also visible in the neutrino-heated ejecta behind the outgoing shock in the successful explosion model of a 13 $\mathrm{M}_\odot$ star computed by Mezzacappa et al. (2000). The neutronization of the neutrino-heated medium is determined by the absorption of ν_e on neutrons and of $\bar{\nu}_e$ on protons and the inverse processes. It is therefore sensitive to the neutrino luminosities, neutrino spectra, and the angular distribution of the neutrinos in the heating region, which govern the efficiency of energy deposition as well as the lepton exchange with the medium.

4. CONCLUSIONS

We have presented results of a Newtonian core collapse simulation in spherical symmetry for a 15 $\mathrm{M}_\odot$ star with a 1.28 $\mathrm{M}_\odot$ iron core. The computation was done with a new Boltzmann solver for the transport of ν_e and $\bar{\nu}_e$ and was carried to 350 ms after core bounce. No explosion was obtained, although the shock reached a larger maximum radius than in a comparable MGFLD simulation. This can be explained by a stronger neutrino heating as was expected for a more accurate treatment of the neutrino transport. Although we have only included ν_e and $\bar{\nu}_e$ in our simulation, we think that our conclusions are solid, because muon and tau neutrinos would drain energy from the ν_e and $\bar{\nu}_e$ luminosities but contribute to the postshock heating only at an insignificant level because of the lack of charged-current interactions. Also general relativistic effects would hamper an explosion.

The importance of an accurate treatment of the ν_e and $\bar{\nu}_e$ transport is emphasized by the interesting finding that $Y_e > 0.5$ in the region of net neutrino energy deposition behind the shock. This is an important result because an electron fraction below 0.49 for the neutrino-heated ejecta was obtained in supernova models, e.g., by Herant et al. (1994), Burrows et al. (1995) and Janka & Müller (1996) (see also Hoffman et al. 1996; McLaughlin, Fuller, & Wilson 1996), causing a severe overproduction of neutron-rich nuclei, in particular in the range of neutron numbers $N \approx 50$ and mass numbers $A \approx 90$ (^{88}Sr, ^{89}Y, ^{90}Zr). This is in conflict with measured galactic abundances. With values $Y_e > 0.5$ this problem disappears.

Using their Boltzmann solver for the neutrino transport, Mezzacappa et al. (2000) obtained a successful, but weak explosion in case of a 13 $\mathrm{M}_\odot$ progenitor star with an extraordinarily small iron core of only 1.17 $\mathrm{M}_\odot$. In case of a 15 $\mathrm{M}_\odot$ star with a larger iron core (and therefore most likely also in case of more massive progenitors), we cannot confirm a qualitative difference from spherically symmetric simulations with MGFLD treatment of neutrinos, although we find important quantitative differences with our more accurate description of the neutrino transport. In order to obtain explosions via the delayed neutrino-heating mechanism, multi-dimensional simulations therefore seem indispensable for stars with typical iron core masses. Convection inside the nascent neutron star (Keil et al. 1996) or lower neutrino opacities — due to suppression relative to the standard description by nucleon correlation effects (e.g., Janka et al. 1996, Reddy et al. 1999, Burrows & Sawyer 1998) — could raise the neutrino luminosities significantly on the relevant time scale of a few hundred milliseconds after core bounce, and convective overturn in the postshock region has been demonstrated by several groups to support the explosion. We shall attempt to do multi-dimensional simulations with our new neutrino transport code, which can be generalized for this purpose relatively easily and permits suitable approximations for efficient computations.

Support by Deutsche Forschungsgemeinschaft grant SFB 375 für Astro-Teilchenphysik is acknowledged. The computations were performed on a NEC SX-5/3C of the Rechenzentrum Garching.

REFERENCES

Bethe, H.A., & Wilson, J.R. 1985, ApJ, 295, 14
Bowers, R.L., & Wilson, J.R. 1980, SSR, 27, 537
Bruenn, S.W. 1985, ApJ Suppl., 58, 771
Bruenn, S.W. 1989a, ApJ, 340, 955
Bruenn, S.W. 1989b, ApJ, 341, 385
Bruenn, S.W. 1993, in *Nuclear Physics in the Universe*, eds. Guidry M.W. and Strayer M.R., Institute of Physics Publ., Bristol, p. 31
Bruenn, S.W., & Dineva, T. 1996, ApJ, 458, L71
Bruenn, S.W., & Mezzacappa, A. 1997. Phys. Rev. D, 56, 7529
Bruenn, S.W., Mezzacappa, A., & Dineva, T. 1995, Phys. Rep., 256, 69
Burrows, A. 1987, ApJ, 318, L57
Burrows, A., & Sawyer, R.F. 1998, Phys. Rev. C, 58, 554
Burrows, A., Hayes, J., & Fryxell, B.A. 1995, ApJ, 450, 830
Burrows, A., Young, T., Pinto, P.A., Eastman, R., & Thompson, T. 2000, ApJ, in press (astro-ph/9905132)
Colgate, S.A., & White, R.H. 1966, ApJ, 143, 626
Fryer, C.L. 1999, ApJ, 522, 413
Fryxell, B.A., Müller, E., & Arnett, W.D. 1989, MPA-Preprint 449, Garching
Herant, M., Benz, W., & Colgate, S.A. 1992, ApJ, 395, 642
Herant, M., Benz, W., Hix, W.R., Fryer, C.L., & Colgate, S.A. 1994, ApJ, 435, 339
Hoffman, R.D., Woosley, S.E., Fuller, G.M., & Meyer, B.S. 1996, ApJ, 460, 478
Janka, H.-Th. 1991, PhD Thesis, TU München, MPA-Report 587
Janka, H.-Th., & Keil, W. 1998, in *Supernovae & Cosmology*, eds. Labhardt L., Binggeli B., and Buser R., Astronomisches Institut der Universit"at Basel, p. 7 (astro-ph/9709012)
Janka, H.-Th., & Müller, E. 1995, ApJ, 448, L109
Janka, H.-Th., & Müller, E. 1996, A&A, 306, 167
Janka, H.-Th., Keil, W., Raffelt, G., & Seckel, D. 1996, Phys. Rev. Lett., 76, 2621
Keil, W., Janka, H.-Th., & Müller, E. 1996, ApJ, 473, L111
Kifonidis, K., Plewa, T., Janka, H.-Th., & Müller, E. 2000, ApJ, 531, L123
Lattimer, J.M., & Swesty, F.D. 1991, Nucl. Phys., A535, 331
Mayle, R., & Wilson, J.R. 1988, ApJ, 334, 909

McLaughlin, G.C., Fuller, G.M., & Wilson, J.R. 1996, ApJ, 472, 440
Messer, O.E.B., Mezzacappa, A., Bruenn, S.W., & Guidry, M.W., 1998, ApJ 507, 353
Mezzacappa, A., & Bruenn, S.W. 1993, ApJ, 405, 637
Mezzacappa, A., Calder, A.C., Bruenn, S.W., Blondin, J.M., Guidry, M.W., Strayer, M.R., & Umar, A.S. 1998a, ApJ, 493, 848
Mezzacappa, A., Calder, A.C., Bruenn, S.W., Blondin, J.M., Guidry, M.W., Strayer, M.R., & Umar, A.S. 1998b, ApJ, 495, 911
Mezzacappa, A., Liebendörfer, M., Messer, O.E.B., Hix, W.R., Thielemann, F.-K., Bruenn, S.W. 2000, Phys. Rev. Lett., subm. (astro-ph/0005366)
Miller, D.S., Wilson, J.R., & Mayle, R.W. 1993, ApJ, 415, 278
Myra, E.S., Bludman, S.A., Hoffman, Y., Lichtenstadt, I., Sack, N., & Van Riper, K.A. 1987, ApJ, 318, 744
Nomoto, K., & Hashimoto, M. 1988, Phys. Rep., 163, 13
Pons, J.A., Reddy, S., Prakash, M., Lattimer, J.M., & Miralles, J.A. 1999, ApJ, 513, 780
Rampp, M. 2000, PhD Thesis, TU München
Reddy, S., Prakash, M., Lattimer, J.M., & Pons, J.A. 1999, Phys. Rev. C, 59, 2888
Wilson, J.R. 1985. In *Numerical Astrophysics*, eds. J.M. Centrella, J.M. LeBlanc, R.L. Bowers, Jones and Bartlett Publ., Boston, p. 422
Wilson, J.R., & Mayle R. 1988, Phys. Rep., 163, 63
Wilson, J.R., & Mayle R. 1993, Phys. Rep., 227, 97
Wilson, J.R., Mayle, R., Woosley, S.E., & Weaver, T. 1986, Ann. NY Acad. Sci., 470, 267
Woosley, S.E., & Weaver, T.A. 1995, ApJ Suppl., 101, 181
Yamada, S., Janka, H.-Th., & Suzuki, H. 1999, A&A, 344, 533

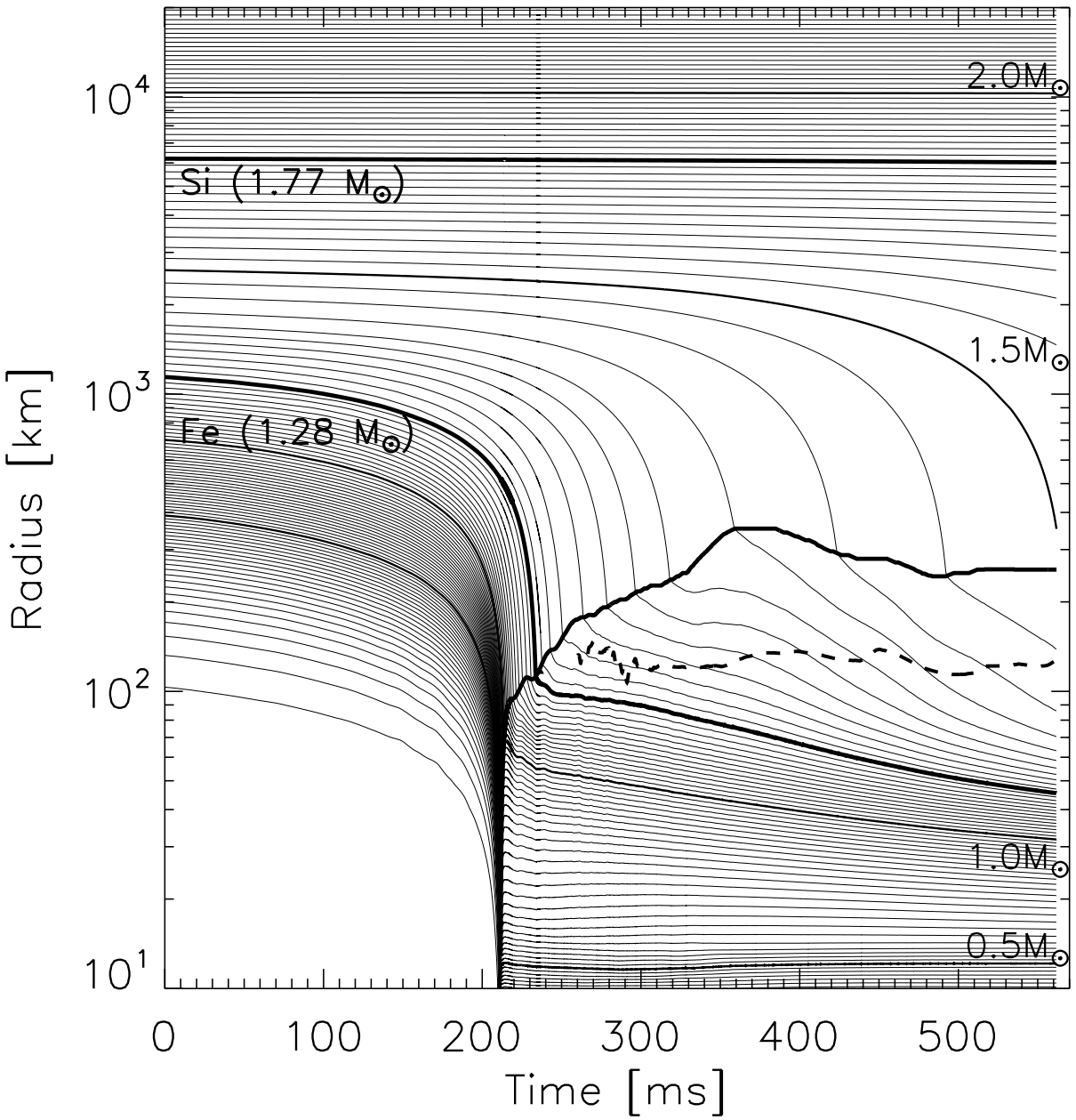

FIG. 1.— Trajectories of selected mass shells vs. time from the start of the simulation. The shells are equidistantly spaced in steps of 0.02 $M_\odot$, and the trajectories of the outer boundaries of the iron core (at 1.28 $M_\odot$) and of the silicon shell (at 1.77 $M_\odot$) are indicated by bold lines. The shock is formed at 211 ms. Its position is also marked by a bold line. The dashed curve shows the position of the gain radius.

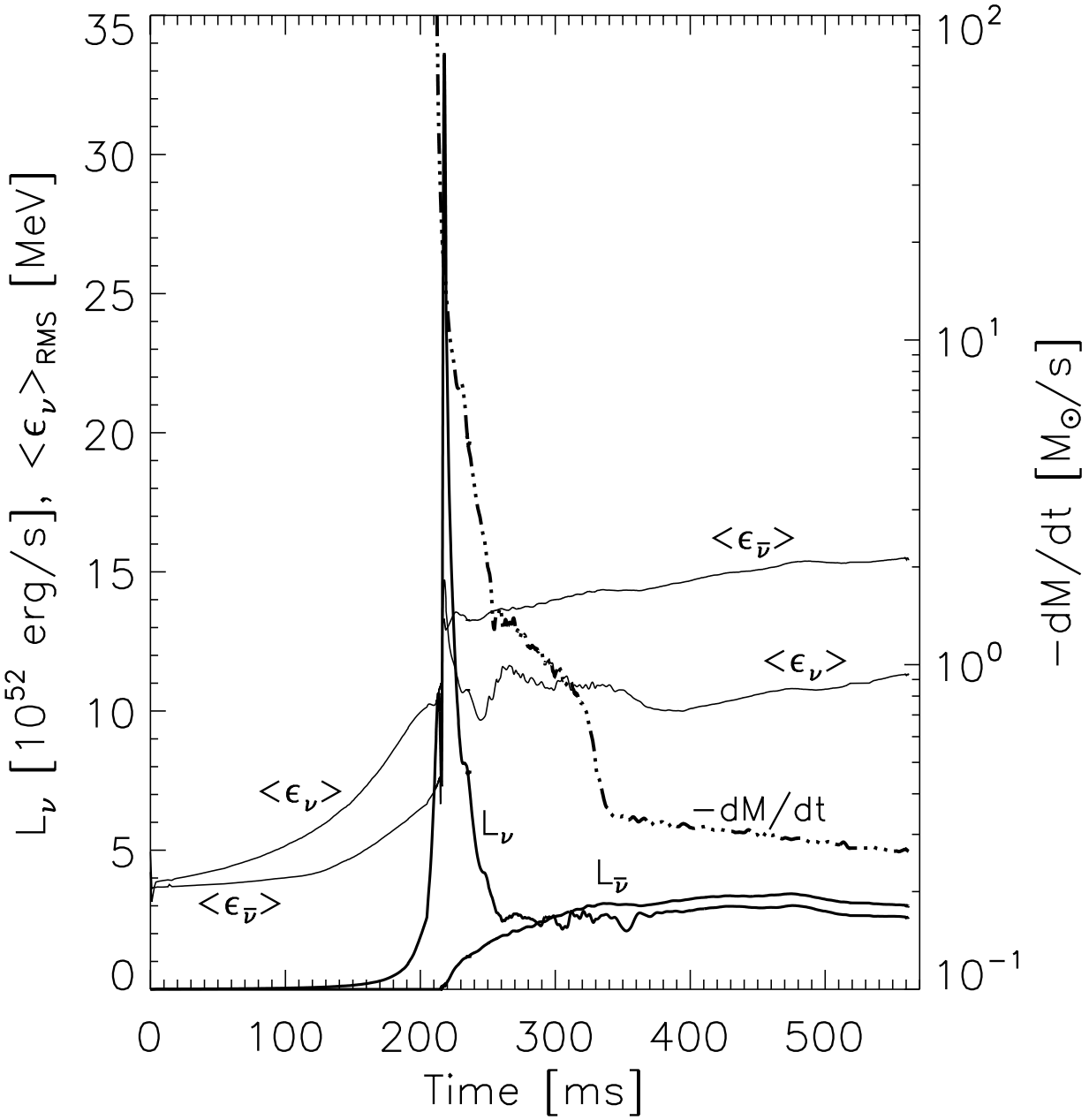

FIG. 2.— Comoving frame electron neutrino and antineutrino luminosities (bold solid lines) and rms energies (thin solid lines) at 1000 km as functions of time. Also shown is the mass accretion rate through the shock (dashed-dotted line, scale on the right ordinate).

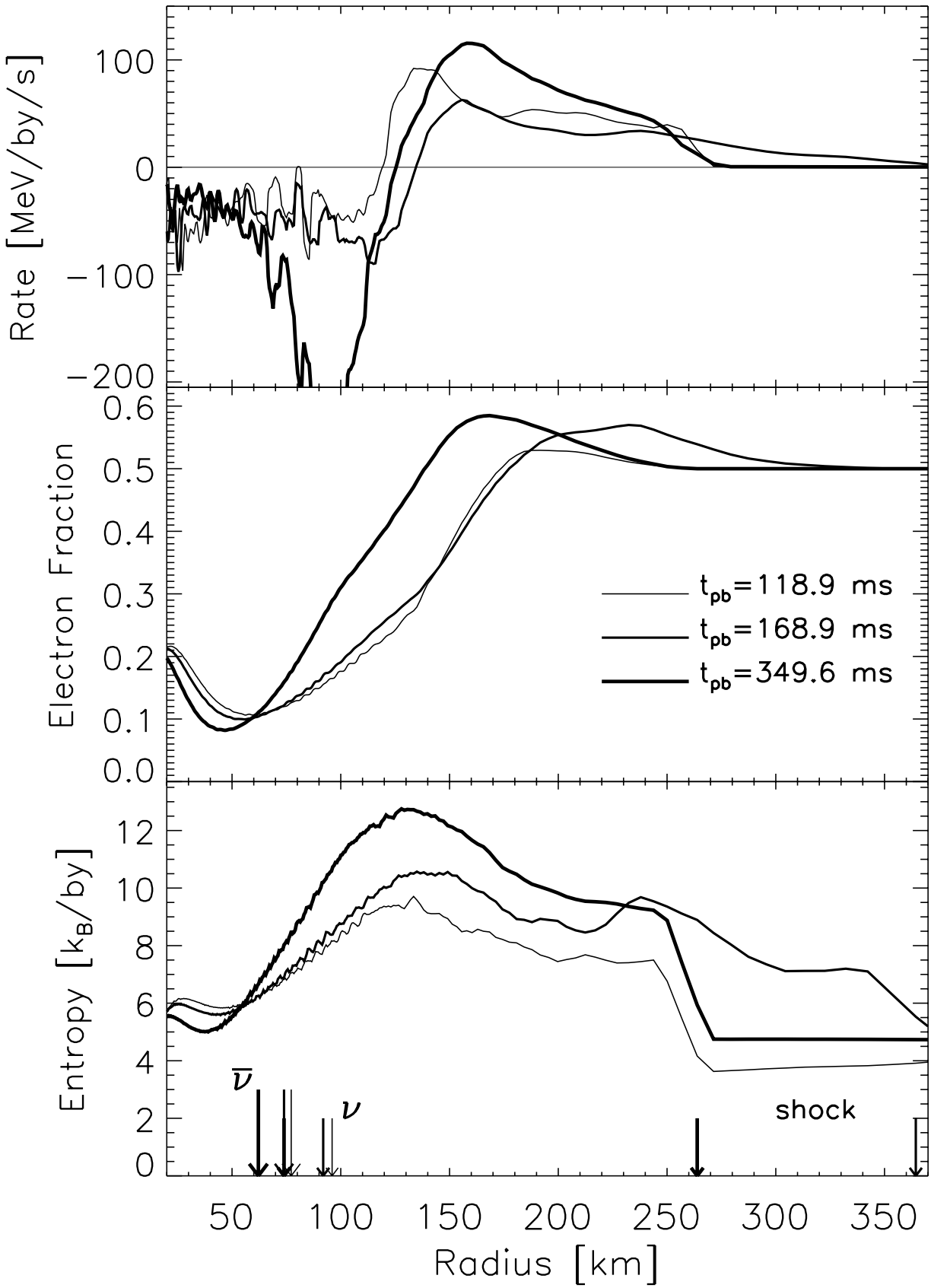

FIG. 3.— Radial profiles of the net energy deposition rate by ν_e and $\bar{\nu}_e$ (top), of the electron fraction (middle) and of the entropy per baryon (bottom) at times 119 ms (thin lines), 169 ms (medium lines) and 350 ms (bold lines) after core bounce. The positions of the shock and of the ν_e- and $\bar{\nu}_e$-spheres are indicated.